

## 62%SiO<sub>2</sub>-32%CaO-6%P<sub>2</sub>O<sub>5</sub> Bioglass as Adsorbent for the Removal of Congo red dye

<sup>1</sup>Virender Yadav\*,<sup>2</sup>Pawan Kumar,<sup>1</sup>D.P.Tiwari,<sup>1</sup>Mamta Bhagat

<sup>1</sup>Department of Chemical Engineering

<sup>2</sup>Department of Materials Science and Nanotechnology  
Deenbandhu Chhotu Ram University of Science and Technology, Murthal

### ABSTRACT

Bioglass is used as cheap and eco-friendly adsorbents for the removal of Congo red dye. It has been studied as an alternative substitute of other adsorbent for the removal of dyes from wastewater. This new bioglass composition consists of 62%SiO<sub>2</sub>-32%CaO-6%P<sub>2</sub>O<sub>5</sub> was successfully prepared by sol-gel method. The various characterization techniques like SEM, TEM, XRD, PSA and FTIR were used to study physicochemical and morphological analysis. The high surface area uniform dispersity enhances the adsorption capacity. The effects of major variables, governing the efficiency of the process such as, contact time, initial dye concentration, bioglass nanoparticle dosage, and pH were investigated. The experimental results have shown that the amount of dye adsorption increased with increasing the initial concentration, dose of adsorbent. The Langmuir and Freundlich adsorption isotherms were used to model the adsorption equilibrium data and it was found that the system followed the Langmuir and Freundlich isotherms. The adsorption capacity of the bioglass nanoparticle was found to be 58% at neutral pH with 150 min.

**Keywords:** Bioglass, adsorption, Congo red, nanoparticles, Langmuir and Freundlich isotherms.

### Introduction

Wastewater is any water that has been contaminated by pollutants such as pathogens, organic and inorganic materials, heavy metals and a wide range of other toxins like dyes. About 10% of diseases worldwide and 6.3% of deaths (largely in developing countries) could be abolished through improvements to the quality of drinking water. Clean water (i.e., water that is free of toxic chemicals and pathogens) is essential to human health and it is a duty of every government to supply clean and healthy water to its citizens. Synthetic dyes have been increasingly used in the textile, paper, rubber, plastic, cosmetics, pharmaceutical and food industries because of their ease of use, inexpensive cost of synthesis, stability and variety of colour compared with natural dyes [2]. Today there are more than 10,000 dyes available commercially. Most of which are difficult to biodegrade due to their complex aromatic molecular structure and synthetic origin. The extensive use of dyes often possess pollution problems in the form of coloured wastewater discharge into environmental water bodies, which interferes with transmission of sunlight into streams therefore reduces photosynthetic activity [3]. A lot of cases throughout the world are reported about the role of dyes in connection with variety of skin, lung, and other respiratory disorders. The presence of dyes in water, even in small concentrations, can be easily detected and can have harmful effects on humans, microbes and other ecosystems as these can also cause inhibitory effects on photosynthesis. The dyes used by the industries have typical characteristics of high degree of stability towards chemical and photolytic degradation and hence these cater to the need of both retailers and consumers. One disadvantage of this stability is that these are not readily degradable under the aerobic conditions established at a sewage treatment plant [3]. Thus, even the colour is removed by chemical and physical methods at the sewage treatment plant and, it may well pass through the receiving water and lead to contamination of water. As the sources of safe drinking water are depleting day by day, new techniques should be developed and used to meet the rising demand of clean water. Various technologies used for the elimination of dyeing effluent include adsorption, coagulation–flocculation, oxidation–ozonation, reverse osmosis, membrane filtration, biological degradation,

solvent extraction and electrochemical processes. The removal of such compounds at such levels consist a difficult problem [6]. The adsorption process provides an attractive alternative treatment, especially if the adsorbent is inexpensive and readily available. Granular activated carbon is the most popular adsorbent and has been used with great success, but is expensive. Consequently, many investigators have studied the feasibility of using low cost substances, such as plum kernels, chitin, chitosan, perlite, natural clay, bagasse pith, fly ash, boiler bottom ash, bagasse fly ash, rice husk, peat, banana pith orange peel, Eichhornia ash, saw dust, walnut shells charcoal, etc. as adsorbents for the removal of dyes from wastewaters. Removal of dyes from an aqueous solution due to its simplicity, high efficiency, easy recovery and the reusability of the adsorbent. In recent times, nanotechnology is widely investigated for different applications related to healthcare and environment. Advances in nanotechnology suggest that many of the current problems involving water quality could be resolved or greatly diminished by using nano adsorbent, nanocatalysts, bioactive nanoparticles, nanostructures catalytic membranes, Nano powder, carbon nanotubes and magnetic nanoparticles [7]. The purpose of this work was to synthesis and investigation of dye removal efficiency of bioglass nanoparticles.

## Material and Method

### Materials

P<sub>2</sub>O<sub>5</sub>, TEOS (tetra ethyl orthosilicate), Calcium nitrate, Citric acid and Ammonium phosphate were purchased from Sigma – Aldrich, India. Congo red dye was purchased from Loba Chemie, India. All the materials used were of analytical grade.

### Synthesis of Bioglass Nanoparticles

TEOS mixed with ethanol and kept on a magnetic stirrer at room temperature for an hour. In this time Calcium nitrate tetra hydrate and phosphorus pent oxide were dissolved in distilled water separately and left on magnetic stirrer for 30 minutes also at room temperature. After one hour calcium containing solution was added to the solution of TEOS. After that phosphorus containing solution added to the mixer solution. Use ammonia solution (25%) to maintain pH 11 of the solution. Transfer the solution to an incubator and kept for 2 days for aging in order to obtain the gel. The aged gel placed in an oven at 100 °C for drying to eliminate ethanol. The dried sample sintered at different temperature for further characterization.

### Characterization Techniques

Particle size and poly dispersity index were determined using a Malvern Zetasizer Nano ZS90 (Malvern Instrument, India) based on quasi-elastic light scattering. This characterization helped in rough estimation of particle size of the nanoparticles. X-ray powder diffraction (XRD) is a rapid analytical technique primarily used for phase identification of a crystalline material and can provide information on unit cell dimensions. The XRD patterns emphasized the predominant crystalline states of the internal disorder and glassy nature of this material feature of the sample. TEM is a microscopy technique in which a beam of electrons is transmitted through a specimen to form an image [7]. FTIR is used to identify certain functional groups in molecules [8].

### Adsorption studies

Different amount of synthesized bioglass nanoparticles were added to 20 ml of 0.05 ppm of dyes (Congo red) solutions followed by magnetic stirring one by one. Different pH (Acidic, neutral and basic) were used for adsorption studies. After equal time intervals, equal amount of samples from stirred solution were taken, centrifuged at 8000 rpm for 5 minutes and absorbance was observed with the help of UV-Visible spectrophotometer. Different pH and different amount of nanoparticles were used for adsorption studies.

$$\text{Dye removal efficiency (\%)} = \frac{C_0 - C}{C_0} \times 100$$

Where, C<sub>0</sub> and C are the initial and absorbance at any time (t) of the dye solution respectively. The adsorption affinity of dyes on the bioglass nanoparticle was determined by the Langmuir and Freundlich isotherm.

## Result and Discussion

### Morphological analysis of Nanoparticle

Particle Size Analyser (Malvern) used for the rough estimation of bioglass nanoparticles. The results obtained are shown in figure 1. The sonicated aqueous solution of nanomaterials was filled in the cuvette and placed in the zeta sizer. The size of bioglass nanoparticles was found to be at around 244.2 nm as shown in below mentioned figure. TEM images of the bioglass nanoparticles presented on Figure 2. TEM is a microscopy technique in which a beam of electrons is transmitted through a specimen to form an image. TEM is a microscopy technique in which a beam of electrons is transmitted through a specimen to form an image [7]. The size of bioglass nanoparticles are found 200 nanometres in size with almost round in shape.

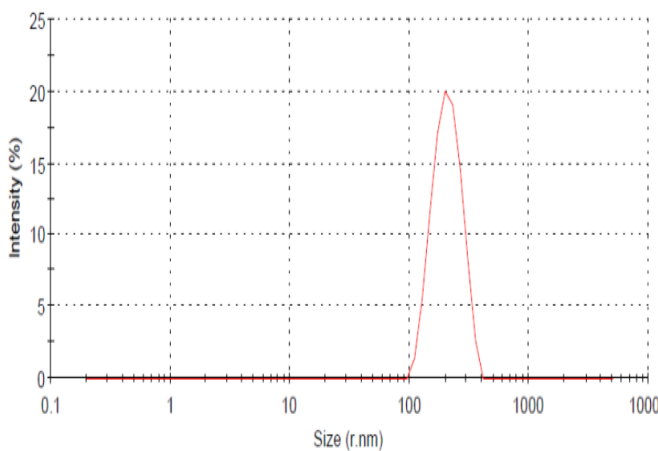


**Fig1. PSA image of bioglass**

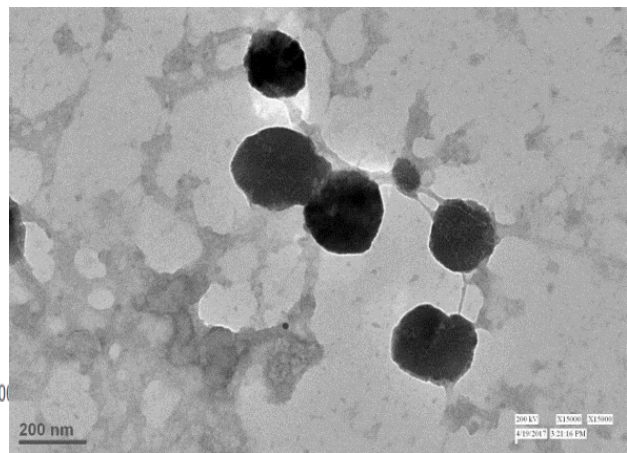


**Fig 2. TEM images Bioglass Nanoparticles**

### Physiochemical Analysis

X-ray diffraction data of the bioglass is presented on Figure 3. The XRD patterns emphasized the predominant crystalline states of the internal disorder and glassy nature of this material feature of the sample [17]. All diffraction peaks could be indexed as the hexagonal structure of 62% SiO<sub>2</sub>-32% CaO-6% P<sub>2</sub>O<sub>5</sub>, which were assigned to (110), (011), (200), (211), (220), (211), (33), (331), (112), (202), (310) etc. planes and were in good agreement with the standard Database PDF-2, Release-2013 (ICDD). Figure 4 shows the FTIR spectrum, in the 500 - 4000 cm<sup>-1</sup> spectral range, of sample. The peak at 587, 798 & 927 1093 cm<sup>-1</sup> were assigned to PO<sub>4</sub><sup>3-</sup> and peak at 467 and 1093 cm<sup>-1</sup> assigned as SiO<sub>2</sub> and peak at 1857 & 1506 assigned CO group and peak at 3400-3600 cm<sup>-1</sup> assigned as OH<sup>-</sup> and peak at 1590 cm<sup>-1</sup> HPO<sub>4</sub><sup>2-</sup> groups.

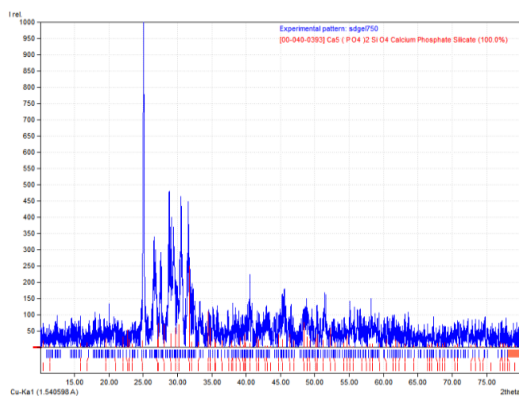


**Fig 3. XRD results of Bioglass Nanoparticles**

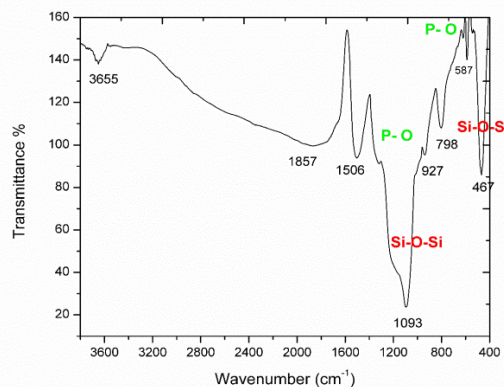


**Fig 4. FTIR Analysis of Bioglass Nanoparticles**

### Adsorption behaviour of bioglass nanoparticles

The above graph shows the maximum % removal of congo red dye at neutral pH more than 58 %. There is comparison among different pH of congo red dyes concentration with 0.1gm nanoparticles. Due to large surface area of nanoparticles, they adsorb more dyes. Above graph show the congo red dye can be removed from wastewater with the help of bioglass nanoparticles. Due to stirring all surface of nonmaterial is exposed and comes in contact with the dye present in aqueous solution, hence rate of dye removal increases.

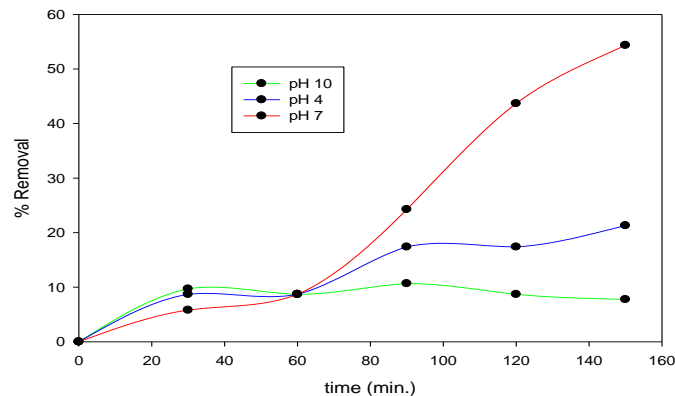


**Fig 5. Comparison of percentage removal of dye at various pH with respect to contact time**

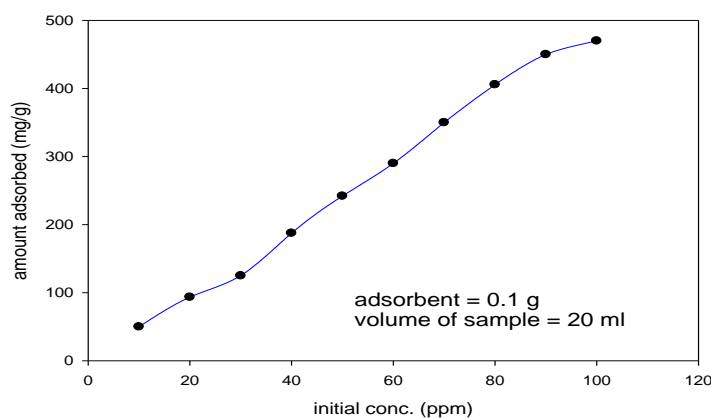


**Fig 6. Effect of concentration on adsorption**

#### Effect of Dye Concentration

The adsorption process at different concentrations at room temperature vs time (2 hrs) was studied. The amount adsorbed of Congo red dye from wastewater is increased with increasing initial concentration (Fig. 6). However, the amount of dye adsorbed per unit of bioglass nanoparticle mass increased as initial dye concentration increased due to the increase in the driving force of the concentration gradient for mass transfer with the increase in initial dye concentration.

#### Effect of Stirring

Stirring is also a critical factor in case of dye removal from waste water. In the absence of stirring whole surface of nanoparticle does not exposed and comes in contact with the dye present in waste water, hence rate of adsorption and dye removal is slow and very much less as compared to the case when stirring is done.

## Adsorption Isotherm

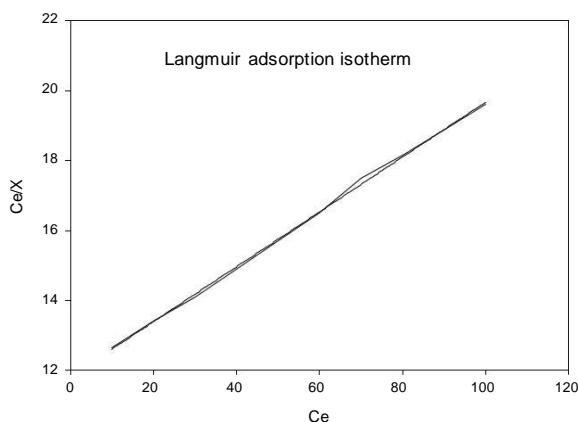


**Fig 7. Langmuir isotherm model**

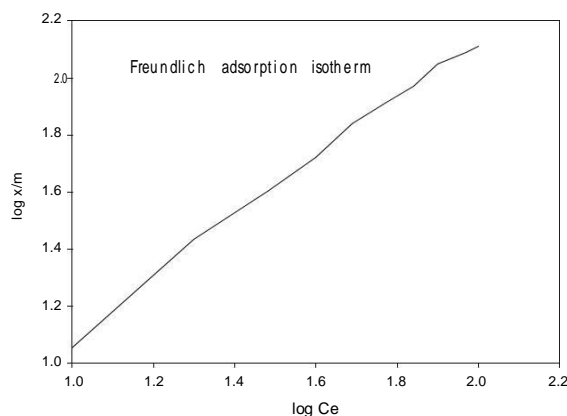


**Fig 8. Freundlich isotherm model**

Where  $x_m$  is the amount adsorbed (mg/g) at concentration  $C$  (mg/g),  $x_m$  is the monolayer adsorption capacity (mg/g) and  $k_L$  (L/mg) and  $k_F$  [(mg/g) (L/mg)<sup>1/n</sup>] are two equation constants related to adsorption energy whereas  $n$  (g/L), in the Freundlich equation is a measure of energetic surface heterogeneity and adsorption intensity. The value of  $R_L$  calculated as per the above equation values lies between 0 to 1 (0.9380) the Langmuir isotherm is favourable.

$$RL = \frac{1}{(1 + KLC_0)}$$

The Freundlich constant  $n$  which should have value in the range of  $0 < n < 1$  for favourable adsorption [17]. Favourable adsorption indicates that all the bioglass nanoparticle have energetically heterogeneous surface. The linear Langmuir and Freundlich adsorption isotherms of Congo red dye on adsorbent are shown in Fig 7 and Fig 8.

**Table. 1 The Langmuir and Freundlich equation constants as calculated from the linear plots are given below**

Sample at temp.	Langmuir isotherm			Freundlich isotherm		
	$X_m$	$k_L$	$R^2$	$n$	$K_f$	$R^2$
40	12.7295	.0066	.9989	0.9693	1.15	0.9958

## CONCLUSION

Bioglass nanoparticles were used as an adsorbent for removal of dye from aqueous solution. The white colour undispersed bioglass nanoparticle were successfully synthesized by sol-gel technique. The maximum removal of congo red dye ions from aqueous solution by bioglass nanoparticle was found to be effective as the adsorption capacity of these adsorbent was 58.8% at neutral pH. The percentage of dye eliminated was found to depend on the pH, initial concentration of dye, stirring and the contact time between dye and adsorbent. The adsorption has been described by Langmuir and Freundlich models. Bioglass nanoparticle hold immense potential as an effective material for waste water treatment for removal of harmful dyes. These nanoparticle can be used as substitute adsorbent for the removal of different dyes from aqueous solution.

---

## References

1. Nirmalya Tripathy , Rafiq Ahmad, JeongEun Song, Hyun Ah Ko, Yoon-Bong Hahn, Photocatalytic degradation of methyl orange dye by ZnO nano needle under UV irradiation, *Materials Letters* 136 (2010) 171-174.
2. Sandeep Kumar, Gaurav Bhanjana, Neeraj Dilbaghi, and Ahmad Umar, Multi Walled Carbon Nanotubes as Sorbent for Removal of Crystal Violet, *Journal of Nanoscience and Nanotechnology* 14 (2014), 1–6.
3. Sandeep Kumar, Gaurav Bhanjana, KavitaJangra, NeerajDilbaghi, and Ahmad Umar, Utilization of Carbon Nanotubes for the Removal of Rhodamine B Dye from Aqueous Solutions, *Journal of Nanoscience and Nanotechnology*, 13 (2013), 1–7.
4. M. Hamadouche, A. Meunier, D.C. Greenspan, C. Blanchat, J.P. Zhong, G.P.L. Torre, L. Sedel, Long-term in vivo bioactivity and degradability of bulk sol–gel bioactive glasses, *J. Biomed. Mater. Res.* 54 (2001) 560–566.
5. H. Arstila, E. Vedel, L. Hupa, M. Hup, Factors affecting crystallization of bioactive glasses, *J. Eur. Ceram. Soc.* 27 (2007) 1543–1546.
6. Sandeep Kumar, Gaurav Bhanjana, Rajesh Kumar, and NeerajDilbaghi, Removal of Anionic Dye Amido Black by Multi-Walled Carbon Nanotubes, *Journal of Nanoengineering and Nanomanufacturing*, 4 (2014) 1–6.
7. O. Peitl, G. La Torre, L.L. Hench, Effect of crystallization on apatite-layer formation of bioactive glass 45S5, *J. Biomed. Mater. Res.* 30 (1996) 509–516.
8. A. Hoppe, N.S. Güldal, A.R. Boccaccini, A review of the biological response to ionic dissolution products from bioactive glasses and glass-ceramics, *Biomaterials* 32 (2011) 2757–2774.
9. ACuneytTas, “Synthesis of biomimetic Ca-hydroxyapatite powders at 37C in synthetic body fluids,” *Biomaterials*, 14 (2000) 1429–1438.
10. J. Ma, C.Z. Chen, D.G. Wang, X.G. Meng, J.Z. Shi, Influence of the sintering temperature on the structural feature and bioactivity of sol–gel derived CaO–P<sub>2</sub>O<sub>5</sub>–SiO<sub>2</sub> bioglass, *Ceram. Int.* 36 (2010) 1911–1916.
11. Q.Z. Chen, G.A. Thouas, Fabrication and characterization of sol–gel derived 45S5 Bioglass ceramic scaffolds, *ActaBiomater.* 7 (2011) 3616–3626.
12. A. Lucas-Grot, F.Z. Mezahi, M. Mami, H. Oudadesse, A. Harabi, M. Le Floch, Sol–gel synthesis of a new composition of bioactive glass in the quaternary system SiO<sub>2</sub>–CaO–Na<sub>2</sub>O–P<sub>2</sub>O<sub>5</sub>: comparison with melting method, *J. Non-Cryst. Solids* 357 (2011) 3322–3327.
13. E. Vedel, D. Zhang, H. Arstila, L. Hupa, M. Hupa, Predicting physical and chemical properties of bioactive glasses from chemical composition. Part 4: Tailoring compositions with desired properties, *Glass Technol.: Eur. J. Glass Sci. Technol., Part A* 50 (2008) 9–16.
14. Sepulveda P, Jones J R and Hench L L 2002 In vitro dissolution of melt-derived 45S5 and sol–gel derived 58S bioactive glasses *J. Biomed. Mater. Res.* 61 (2002) 301–11.
15. A.O. Dada, A.P. Olalekan, A.M. Olatunya, O. DADA, Langmuir, Freundlich, Temkin and Dubinin–Radushkevich Isotherms Studies of Equilibrium Sorption of Zn<sup>2+</sup> Unto Phosphoric Acid Modified Rice Husk, *Journal of Applied Chemistry*, 3 (2012), 38-45.
16. Doostmohammadi A, Monshi A, Salehi R, Fathi M H, Golniya Z and Daniels A U Bioactive glass nanoparticles with negative zeta potential *Ceram. Int.* 37 (2011) 2311–6.
17. M. Sarioglu and U.A. Atay, Removal of methylene blue by using biosolid, *Global NEST Journal*, 8 (2006), 113-120.
18. Palin E, Liu H N and Webster T J Mimicking the nanofeatures of bone increases bone-forming cell adhesion and proliferation *Nanotechnology* 16 (2005) 1828–35.
19. Schneider O D et al Cotton wool like nanocomposite biomaterials: in vitro bioactivity and osteogenic differentiation of human mesenchymal stem cells *J. Biomed. Mater. Res. B: Appl. Biometer.* 84 (2008) 350–62.
20. Elvis Fosso –Kankeu, Frans Wannders, and Maryka Geldenhuys, photocatalytic degradation of dyes using TiO<sub>2</sub> Nanoparticles of different shapes, 7<sup>th</sup> international conference on latest trends in engg. & technology, (2015) 26-27.